journal of the American Ceramic Society

Deformation-resistant $Ta_{0.2}Hf_{0.8}C$ solid-solution ceramic with superior flexural strength at 2000°C

Journal:	*Journal of the American Ceramic Society*
Manuscript ID	JACERS-47914.R1
Manuscript Type:	Research Article
Date Submitted by the Author:	n/a
Complete List of Authors:	Demirskyi, Dmytro; Tohoku Daigaku, Advanced Institute for Materials Research (AIMR) Borodianska, Hanna; National Institute for Materials Science, Advanced Materials Processing Unit Nishimura, Toshiyuki; National Institute for Materials Science, Nano Ceramics Center Suzuki, Tohru; National Institute for Materials Science, Research Center for Functional Materials Yoshimi, Kyosuke; Tohoku University, Department of Materials Science and Engineering VASYLKIV, Oleg; National Institute for Materials Science, Research Center for Functional Materials
Keywords:	strength, ultra-high temperature ceramics, spark plasma sintering
Author-supplied Keyword: If there is one additional keyword you would like to include that was not on the list, please add it below::	tantalum hafnium carbide

Deformation-resistant $Ta_{0.2}Hf_{0.8}C$ solid-solution ceramic with superior flexural strength at 2000 °C

D. Demirskyi (a,b,c)†, H. Borodianska (b) , T. Nishimura (b), T.S. Suzuki(b), K. Yoshimi (c), O. Vasylkiv (b)†.

(a) WPI-Advanced Institute for Materials Research (WPI-AIMR), Tohoku University, 2-1-1 Katahira, Aoba-ku, Sendai, 980-8577 Japan
(b) National Institute for Materials Science, 1-2-1 Sengen, Tsukuba, Ibaraki 305-0047, Japan
(c) Department of Materials Science and Engineering, Tohoku University, 6-6-02 Aramaki Aza Aoba, Sendai, 980-8579, Japan

In this study we explored the consolidation, solid-solution formation and high-temperature properties of tantalum hafnium carbide with the 1 TaC:4 HfC ratio, i.e., $Ta_{0.2}Hf_{0.8}C$. Tantalum hafnium carbide bulks can be consolidated using spark-plasma sintering only at temperatures exceeding 2200 °C. The bulks prepared using a 40-min dwell at 2200 °C had the lattice parameter a = 4.571(9) Å. Based on the three-point flexural tests, it was observed that the toughness and strength of $Ta_{0.2}Hf_{0.8}C$ remained high at 2000 °C (3.4±0.4 MPa $m^{1/2}$, 500±20 MPa). At 2000 °C, the majority of carbides shows a plastic behavior, but the strain-stress curves of the SPSed $Ta_{0.2}Hf_{0.8}C$ ceramic were linear. Using the shrinkage rate data during the SPS and the strain-stress data from the high-temperature flexure, we estimated the

† Authors to whom correspondence should be addressed, Dmytro Demirskyi, demirskyi.dmytro.e2@tohoku.ac.jp, Oleg Vasylkiv oleg.vasylkiv@nims.go.jp

activation energies for the densification and flexure as 820±20 kJ/mol and 1180±120 kJ/mol, respectively.

Keywords: tantalum hafnium carbide; flexural strength; ultra-high temperature ceramics; spark plasma sintering.

1 Introduction

Recent interest in high-temperature materials has increased the interest in the research of ultra-high temperature ceramics (UHTC) which are known to have extremely high melting points above 3000 °C [1–3]. Within typical carbide UHTCs, the TaC – HfC binary system still has the highest known measured melting point (>3990 °C) [4,5]. Thus it is not surprising that studies were undertaken to produce bulk specimens in the TaC–HfC system. This was because of the high-melting point of the solid-solution carbide densification and the formation of the binary solid-solution requiring temperatures exceeding 2000 °C [5].

The study of Barraza et al. [5] observed that at room temperature the 1:4, 1:1 and 4:1 HfC–TaC ceramics had high elastic moduli (450–550 GPa) and a moderate hardness up to 20 GPa. Furthermore, of the three solid-solutions, the 1TaC:4HfC ($Ta_{0.2}Hf_{0.8}C$) solid-solution had the highest toughness of 3.4±0.6 MPa $m^{1/2}$, exceeding the toughness reported for the monolithic TaC [5,6]. Nevertheless, because of the exposure to temperatures above 2000 °C using spark-plasma sintering

(SPS), the grain growth control and achieving a density exceeding 98% of the theoretical density remain a challenge. This limits the data on potentially good high-temperature strength. Considering good high-temperature compressive creep [7], one may expect that the properties, such as high-temperature toughness or flexural strength for the TaC–HfC system, will also be superior to the monolithic HfC or TaC bulks as it is expected that solid-solution strengthening will play a role in determining the strength at elevated temperatures [8–10].

In this study, we focused on the consolidation and high-temperature strength and toughness of the $Ta_{0.2}Hf_{0.8}C$ ceramics prepared by the SPS method using commercially-available powders. For this purpose, specimens with a diameter of 30-mm and height of 6 mm were consolidated using SPS consisting of a two-step consolidation process in which a lengthy dwell was applied at 1800 °C and 2200 °C.

2 Materials and Methods

Commercially-available HfC (Alfa Aesar, Lot #W19E52) and TaC (Wako Pure Chemical Industries, Lot #LKP4101) powders were used as the starting materials. The received untreated powder was used for consolidation by the spark plasma sintering (SPS) method using a 1:4 molar ratio between TaC and HfC. The SPS experiments were conducted using the 'Dr. Sinter' 1050 (Sumitomo, Japan) unit with a 30-mm die, and as a rule, 40 to 42 g batches were produced.

The schedule for the hafnium carbide specimens prepared in this study had four major steps: (1) heating to 900 °C in four minutes following (2) a 50 °C/min heating to the densification temperature within 1800 °C. At 1800 °C, a dwell of 40 min was used as a homogenizing step. The temperature was then increased to 2200 °C at a rate of 200 °C/min. The dwell between 20 and 40 minutes at 2200 °C was used. The final step included cooling to 600 °C in 40 minutes. The pressure of 34 kN was maintained during the consolidation and cooling stages. Argon gas at the flow rate of 2 L/min was used.

An X-ray diffraction (XRD) analysis (D8 Advance, Bruker, Karlsruhe, Germany) was performed on the polished surfaces of the bars after the flexural tests using Cu-Kα radiation. The intensity data were collected over the 2θ range of 20°–145° in steps of 0.02–0.05° using a sampling time of 10 s for each step. The software used for refinement was TOPAS (TOPAS Ver. 4.2, Bruker AXS, Germany). Instrumental broadening was determined using a NIST 660b LaB_6 standard run under the same conditions for each carbide sample.

The structural characteristics of the tantalum hafnium carbide ceramics were studied by scanning electron microscopy (SEM, JCM-6000, JEOL) with secondary electrons (SE) or backscattered electrons (BSE mode).

The three-point flexural strength was determined using rectangular blocks (2 mm×2 mm×25 mm, 2 mm×2.5 mm×25 mm) and the strength testing equipment

that was previously described in detail [11]. A span of 16 mm was used. The fracture toughness of the ceramics was evaluated by the specimen bending testing which contained a single edge through-thickness notch following ASTM C1421–10. Toughness was tested in the same direction as the pressure was applied during the SPS consolidation. Details of the testing configuration and the notch profile were presented in ref. [12].

To evaluate the strain dependence of the yield stress [13] for the tantalum hafnium carbide, tests were performed using loading rates of 0.1 to 25 mm/min (1800 °C–2000 °C). We selected the loading rate to have the two orders of magnitude difference between the minimum and the maximum loading rates. The effect of the loading rate on the flexural strength below 1800 °C was minimal as data were within the statistical variation for the rate of 0.5 mm/min. Tests below 1800 °C were performed at the loading rate of 0.5 mm/min. Tests at elevated temperatures were performed in argon [11].

The hardness was determined by an MMT-7 Vickers hardness tester (Matsuzawa MMT-7; Matsuzawa SEIKI Co., Ltd., Tokyo, Japan) using loads of 9.8 N and 98 N with a dwell time of 15 s following the standard procedure (ASTM C 1327–15).

3 Results and Discussion

3.1 Consolidation of tantalum hafnium carbide

Figure 1 shows details of the non-isothermal runs of the powder mixture at a heating rate of 50 °C/min and a constant pressure of 24 kN. It can be seen that the maximum shrinkage and noticeable shrinkage rate were observed only above 2200 °C. There was a minor peak at 1600 °C, which can be attributed to a particle rearrangement or initial reaction between the HfC and TaC. Following non-isothermal runs, the lattice parameter of the solid-solution carbide was evaluated as $a = 4.56$ Å. The relative density of the bulks remained below 92% of the theoretical density evaluated by the XRD data.

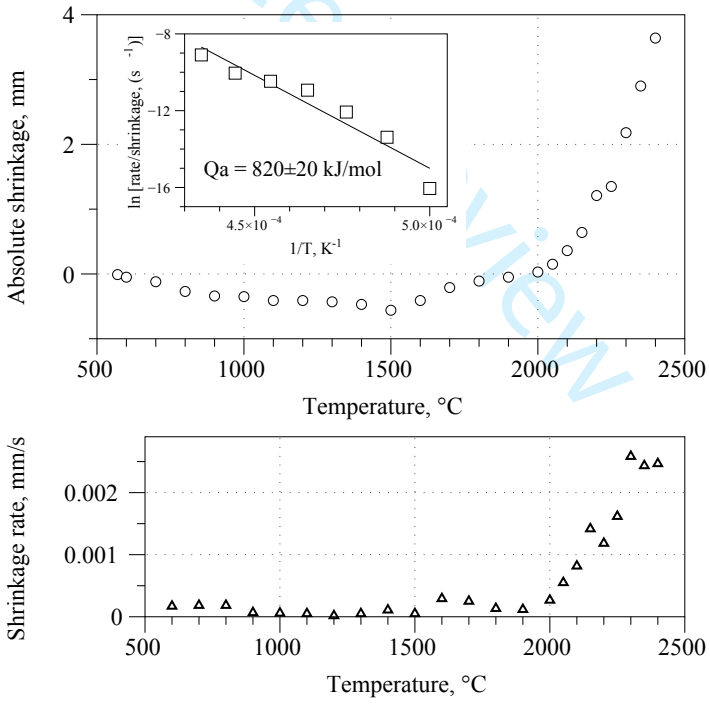

Figure 1. Details of shrinkage behavior of the powder compact via constant rate heating experiments during spark-plasma consolidation of $Ta_{0.2}Hf_{0.8}C$.

Because of the uncertainty of the elastic modulus vs porosity data for the solid-solution carbide, one cannot use the typical model for the hot-pressing [14]. Thus, assuming a number of oversimplifications using the shrinkage and shrinkage rate data, one may estimate an activation energy for the shrinkage from the SPS data using a method applied in [14,15]. A plot of the shrinkage rate vs 1/T would yield an activation energy for the non-isothermal SPS runs. The activation energy for the densification based on the slope for this zone was estimated in **Fig. 1**. The apparent activation energy (n*Q) was 410 ± 10 kJ/mol. Within a close approximation, the activation energy of the densification process can be evaluated using *n* equal to 1/2 and 1/3 for the volume or grain-boundary diffusion [16]. Although the model in [16] was developed for conventional sintering, in the case of SPS and constant pressing conditions, the shrinkage data can be analyzed using the conventional (pressureless) sintering equations [13]. If volume diffusion kinetics predominate, the activation energy, Q, is 820±20 kJ/mol, which is reasonable considering the creep data in [7] for $Ta_{0.25}Hf_{0.75}C_{0.94}$. Grain-boundary diffusion kinetics give 1230±30 kJ/mol, in poor agreement with the previously reported values of 855±85 kJ/mol ($Ta_{0.25}Hf_{0.75}C_{0.94}$) and 780±70 kJ/mol ($Hf_{0.5}Ta_{0.5}C_{0.93}$) [7]. This mechanism should not dominate for carbide ceramics with coarse grain size (24±8 μm).

Figure 2 illustrates the effect of the dwell time on the relative density and on the lattice parameter for the $Ta_{0.2}Hf_{0.8}C$ ceramic. After reaching a 30-min dwell, the

lattice parameter for the solid-solution phase remained unchanged. This observation is consistent with an earlier study [5]. At the same time, the relative density shows a gradual increase with the dwell, however, when the dwell exceeded 40 minutes, a decrease in the relative density was observed. This can be interpreted as dedensification as a result of the ongoing grain-growth process. When the grains grow, the larger grain clusters may create voids leading to the density decrease [17].

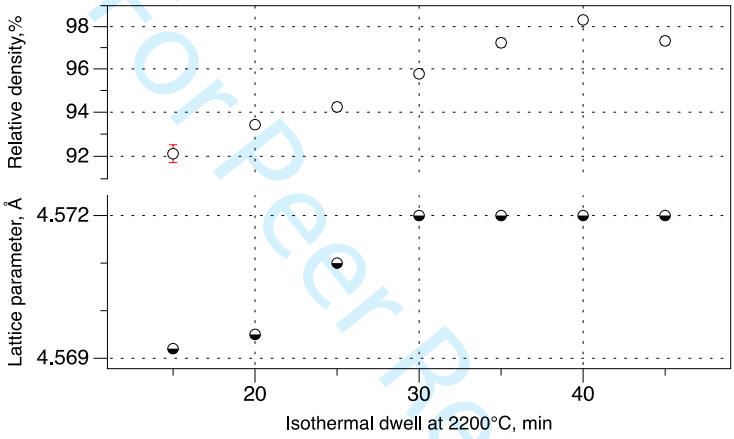

Figure 2. Effect of dwell at 2200 °C on the relative density and lattice parameter of the $Ta_{0.2}Hf_{0.8}C$ ceramics consolidated using SPS.

For the mechanical properties at the elevated temperatures, we selected the $Ta_{0.2}Hf_{0.8}C$ bulks with a relative density of 98.3±0.1 % of the theoretical density (TD) (**Figure 2**). This specimen had a mean grain size value of 24±8 μm measured by SEM using ImageJ and the data-set of >5000 grains using images of polished and fractured specimens.

3.2 Solid-solution formation for tantalum hafnium carbide

Figure 3 shows the XRD data for the bulk HfC, TaC and $Ta_{0.2}Hf_{0.8}C$ carbides prepared within this study. A slight texture for the solid-solution carbide can be seen from the X-ray data as patterns were normalized using the peak with the highest intensity, i.e., (111). Furthermore, one can expect that line broadening and absence of a clear $K_{\alpha 2}$ peak for the TaC or $Ta_{0.2}Hf_{0.8}C$ ceramics is due to the local strain and crystallite size distribution. **Figure 4** summarizes the Rietveld refinement of the tantalum hafnium carbide. The refined lattice parameter was $a = 4.5719$ Å. **Figure 5** illustrates the lattice parameter data in the TaC–HfC system using the data from [4,5,7].

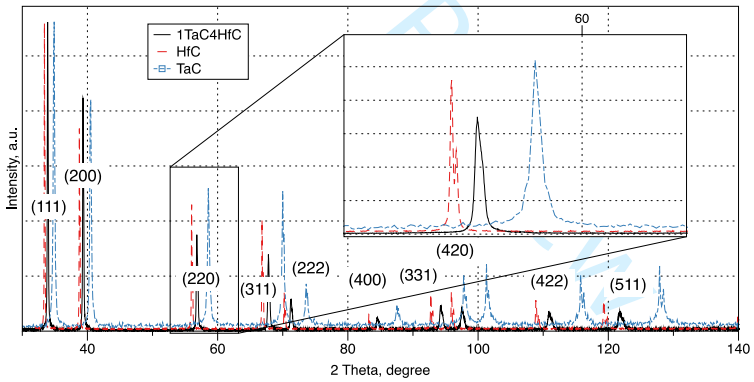

Figure 3. X-Ray diffraction details of bulk tantalum hafnium carbide when compared to the original TaC and HfC powders. The peak intensity was normalized to the first peak.

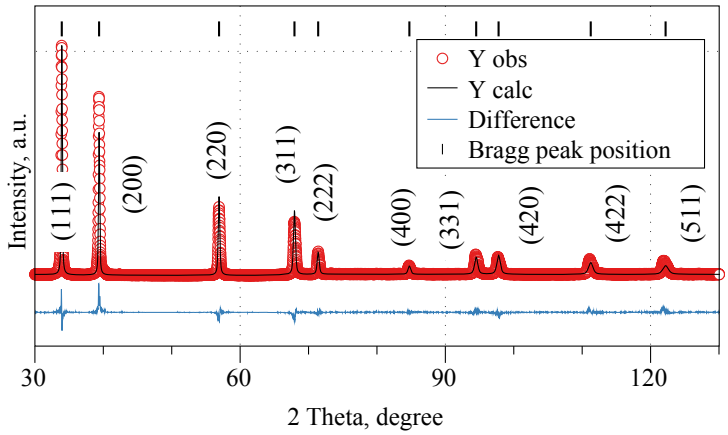

Figure 4. Results on refinement of the $Ta_{0.2}Hf_{0.8}C$ bulks using the lattice parameter of 4.5719 Å.

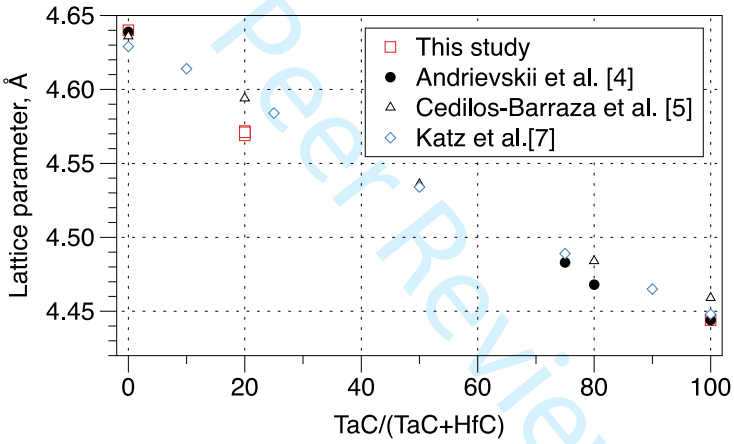

Figure 5. The lattice constant of the solid-solution carbides in the TaC–HfC as a function of the TaC content [4,5,7].

3.3 Mechanical properties and fracture peculiarities

The macroscopic hardness for the bulk ceramics from the TaC–HfC system were reported in several studies [4,5,17–19]. However, the majority of the early tests were made using micro-loads from 50 to 200 g-force (0.49 N to 1.96 N). Loads exceeding

9.8 N were used in the present study and the hardness of $Ta_{0.2}Hf_{0.8}C$ was found to be 18.4±0.8 GPa. However, at 98 N, the hardness averaged 16.2±1.4 GPa. This value is in close agreement with the data of Silvestroni et al. [6] for HfC.

Figure 6 shows the flexural strength and fracture toughness as a function of the temperature. The strength shows two minima when analyzed vs temperature. The first minimum is observed at 600 °C, where it is most likely that the strength decrease is associated with the release of thermal stresses [20]. Such stresses are usually formed during cooling from high temperature, and upon reheating [20,21], these may relax and cause a change in the strength or toughness [22]. The second minimum was observed at 2000 °C. At this temperature, the majority of the carbides is expected to be fractures with some degree of plasticity. The strain-stress curves for specimens tested at 2000 °C were linear without any signs of plasticity. Recall that a noticeable shrinkage rate during consolidation of this carbide was observed only above 2000 °C. Hence, it is possible that plastic deformation may happen only at the tip of the crack wake, since a slight increase in the fracture toughness was observed at 2000 °C.

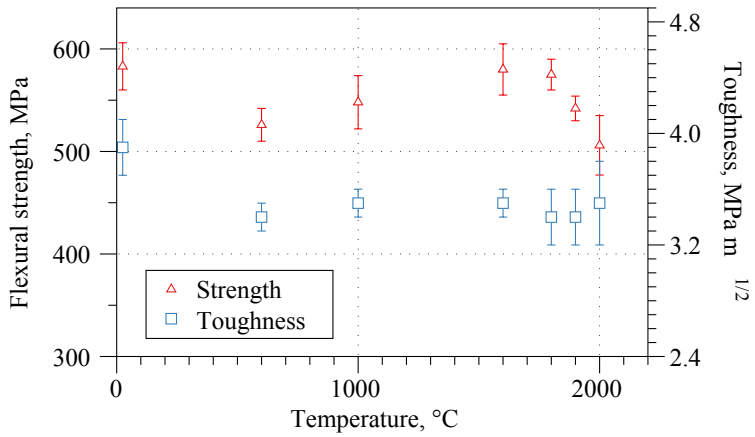

Figure 6. Flexural strength and fracture toughness of $Ta_{0.2}Hf_{0.8}C$ as a function of the testing temperature.

Fracture details for the specimens after the high-temperature flexural tests are summarized in **Figure 7**. Up to 1800 °C, the striations that indicate a typical 'brittle' fracture were observed. At 1600 °C, for example, striations were observed in ~40% of the grains that were fractured according the transgranular mechanism. Intergranular fracture was a dominant fracture mechanism at room temperature and was controlling the fracture behavior of the $Ta_{0.2}Hf_{0.8}C$ specimens up to 2000 °C. At this temperature only few large-sized grains were fractured in the transgranular manner (34 grains from 2312 analyzed grains, i.e. 1.4%).

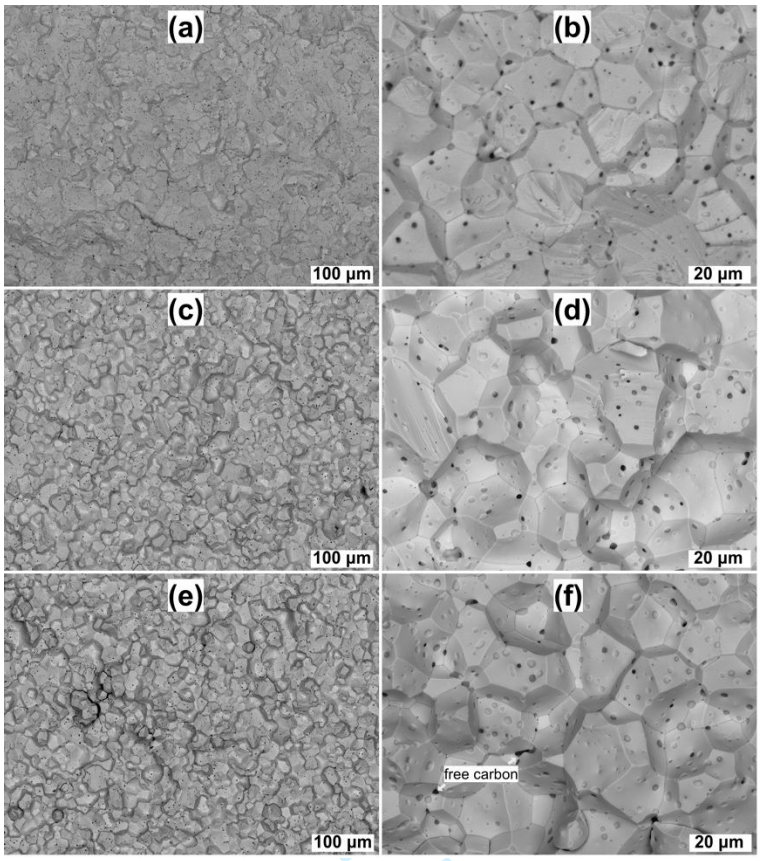

Figure 7. Representative microstructures of the $Ta_{0.2}Hf_{0.8}C$ ceramics following the flexural strength tests at (a,b) room temperature, (c,d) 1600 °C, and (e,f) 2000 °C. One can notice that fractured grains would have a dark grey phase (BSE mode) with a size of up to 2 µm and fine pores. This phase was identified as Ta-rich HfO_2 by EDS (see *Supplementary data*). The contribution of oxide and pores following the SEM analysis using ImageJ was considered to be 1.2% oxide and 1.1–1.3% pores, which is in agreement with the relative density for the as-SPSed specimens (**Figure 2**).

3.4 Effect of composition and solid-solution on fracture toughness

Figure 8 shows variation of the fracture toughness in the TaC–HfC system as a function of the TaC content. One can see that for the monolithic tantalum carbide, the fracture toughness changes from 2.5 to 3.9 MPa $m^{1/2}$ [6,23]. On the contrary, the toughness of the monolithic hafnium carbide lies between 1.3 and 3.5 MPa $m^{1/2}$ [19,24]. A specially prepared equimolar composition would yield a toughness of 3.1 MPa $m^{1/2}$, while Cedilos-Barraza et al. [5] reported a toughness of 2.9±0.7 MPa $m^{1/2}$.

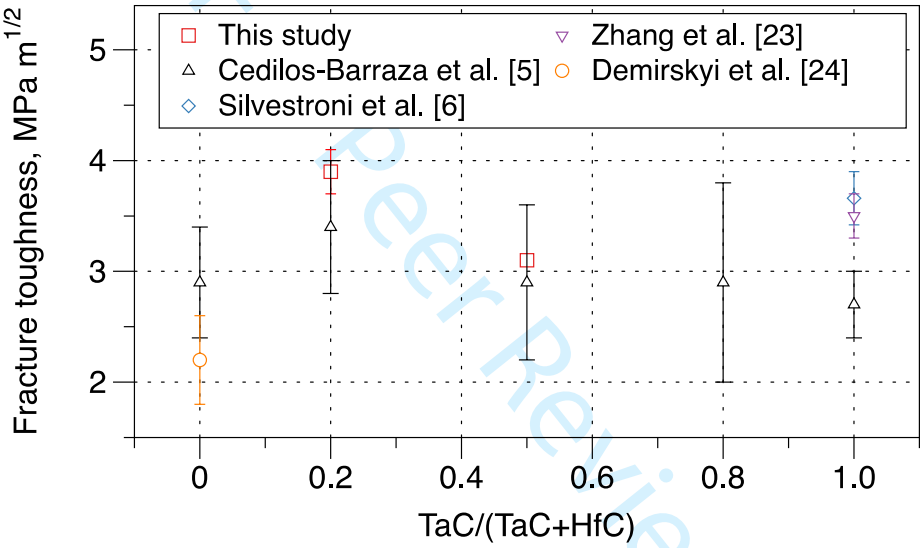

Figure 8. Effect of the TaC addition on fracture toughness in the TaC–HfC system.

The toughness of the $Ta_{0.2}Hf_{0.8}C$ carbide was comparable to that for tantalum carbide and the highest toughness observed was 4.1 MPa $m^{1/2}$. The toughness value for $Ta_{0.2}Hf_{0.8}C$ can be attributed to the high relative density. In this case, oxide particles may cause a local stress concentration leading to a crack deflection. In addition, the formation of the solid-solution may contribute to the increase in toughness as formation of a solid-solution is known to cause stresses at the lattice level [8]. If

such a mechanism is valid at room temperature, with an increase in the temperature up to 1400 °C [20,21], stresses should be relaxed and, as a result, the toughness should decrease. The data in **Figure 6** show that the toughness between 600 °C and 2000 °C is within 3.4±0.2 MPa $m^{1/2}$, which is lower than at room temperature 3.9±0.2 MPa $m^{1/2}$. The high temperature dependence of toughness is nearly insensitive to temperature. This can be explained by a number of factors, but we consider that intensive testing (i.e., more than 4 points per temperature as in this study) may provide additional clarification.

3.5 High-temperature flexural strength

Figure 9 summarizes the high-temperature strength for selected ultra-high temperature solid-solution carbides including data for the high-entropy carbide ceramics [25–28]. Data . One can see that for data from past studies [25,26], the flexural strength increases up to 1600 °C, then will decrease to a ~ 200 MPa range. This value will vary based on a number of factors including the strain rate. For instance, the 180 MPa at 2000 °C was observed using a loading rate of 0.5 mm/min in [26], while 320 MPa in [25] was observed using a loading rate of 2.5 mm/min. In both studies, the strain-stress curve for specimens had a shape typical for ceramics that fracture in the plastic manner (i.e., quasi-sigmoidal shape with a significant deviation from the initial elastic part). Density, grain size, and preparation method

are among the factors that may control the flexural strength (see **Table 1** or original studies for details).

For $Ta_{0.2}Hf_{0.8}C$ in this study, data for the loading rate of 0.5 mm/min are being used in **Figs. 6** and **9**. Similar to the results for some monolithic carbides [13] one can gain additional details on the high-temperature deformation of carbide ceramics by analyzing the strain-stress curves as a function of the loading rate (see *section 3.6*).

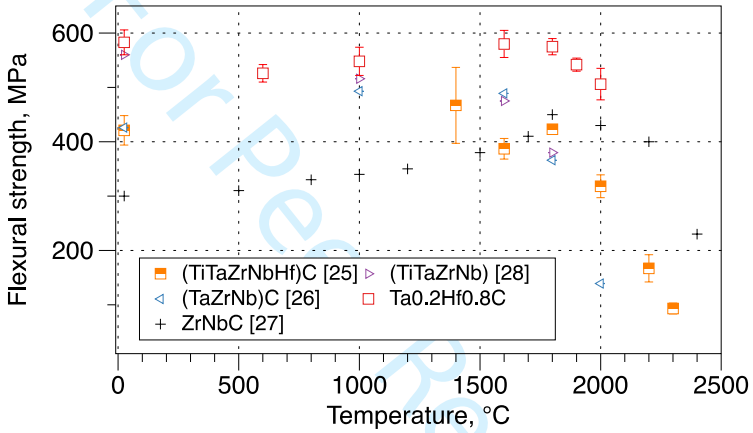

Figure 9. Effect of temperature on flexural strength of selected ultra-high-temperature carbides [25–28].

Using the schedule presented for bulk $Ta_{0.2}Hf_{0.8}C$, i.e., 2200 °C for 40 min, we performed screening of the nearby area to the 20 mol.% TaC for the possible maxima in the flexural strength at 2000 °C. In general, the **Figure 10** [24,29] data for these specimens were lower or within the values measured for the $Ta_{0.2}Hf_{0.8}C$. Note that the number of specimens used for the screening of the 2000 °C strength was limited by two per composition as these were tested within a single testing load of 12

specimens. This number is the maximum value possible using the high-temperature strength facility available at NIMS [11]. Based on these tests, the highest value was measured for the $Ta_{0.17}Hf_{0.83}C$ composition (512 MPa, lattice parameter $a = 4.581$ Å). Note that the highest reported testing temperature reported for monolithic tantalum carbide was remeasured at 1600 °C [29]. Considering the absence of 2000 °C data for TaC, we tested specimen prepared in [29] at 2000 °C.

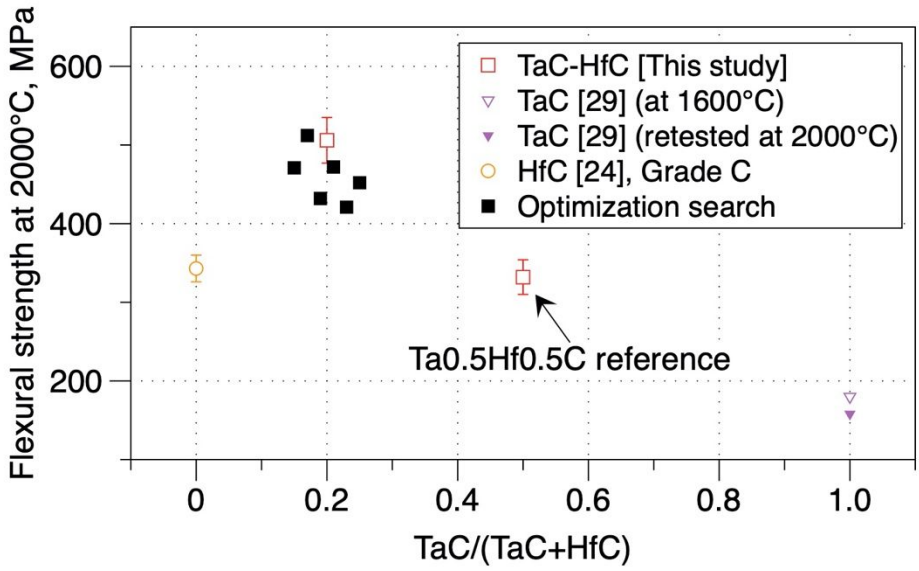

Figure 10. Effect of TaC addition on the flexural strength at 2000 °C of the monolithic and solid-solution carbides in the TaC–HfC system.

Figure 11 shows a polished cross-section of the $Ta_{0.2}Hf_{0.8}C$ ceramic following a 0.5 mm/min test. It was highly likely that the surface flaw was responsible for the crack nucleation. However, one can see that at 2000 °C, crack propagation arrests at several sites as well as changing the crack growth direction (deflection). The inset indicates a place were a crack goes beyond a polished cross-section. Another

peculiarity is that there is a considerable number of grain pull-out sites that may contribute to additional energy consumption during the crack propagation.

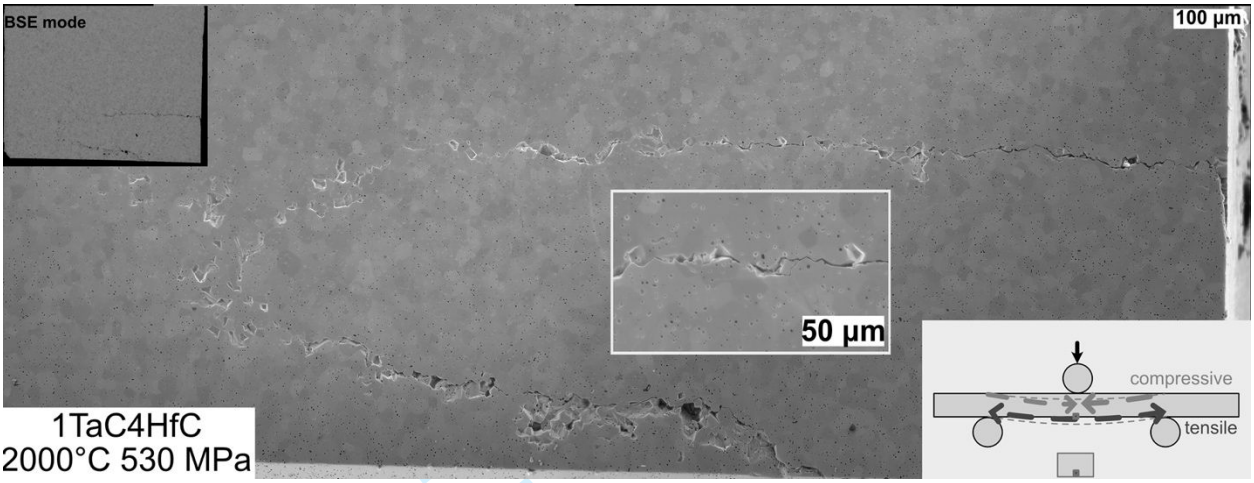

Figure 11. Crack propagation during the flexural testing at 2000 °C for $Ta_{0.2}Hf_{0.8}C$ ceramic. Insets show a macroscopic view of the polished cross-section in the BSE mode and enlarged section of the crack arrest inside a carbide grain.

3.6 Effect of loading rate on high-temperature deformation

In order to obtain additional high-temperature deformation data of the monolithic tantalum hafnium carbide specimens, we attempted to determine the yielding behavior of the $Ta_{0.2}Hf_{0.8}C$ at different strain rates. Previously, it had been mentioned that different carbide ceramics may have a different dependences on the strain rate [13,30]. Darolia and Archbold [13] reported that for polycrystalline zirconium carbide, a positive variation of a 0.2 yield strength may allow one to estimate the activation energy for the carbide at elevated temperatures. The methodology

proposed in [13] requires performing strength tests with different strain rates (loading rate). In this study, we selected the loading rate to ensure the two orders of magnitude difference between the minimum and the maximum loading rates. If there is a linear increase in the 0.2 yield strength vs loading rate, one can evaluate the activation volume of deformation as

$$V = kT\frac{\Delta \ln \dot{\varepsilon}}{\Delta \sigma},$$

where k is the Boltzmann constant, T is the absolute values of the temperature of the test, $\dot{\varepsilon}$ is the plastic strain rate, and σ is the yield strength.

Figure 12 shows the dependence of the yield strength of the $Ta_{0.2}Hf_{0.8}C$ carbide as a function of the strain rate at 2000 °C. The activation volume can be obtained by plotting the yield strength vs logarithm of the strain rate (**Figure 13**). The evaluation of the activation volume at 2000 °C yields a value of 481 Å^3. Assuming the lattice parameter from the XRD measurements as a = 4.5719 Å, one can expect that such a volume is proportional to ~40**b**^{3} (**b** is a a/2 [1-10]. For clarity, the tantalum carbide values of 50**b**^{3} to 55**b**^{3} have been reported [31], while the HfC data yielded ~30**b**^{3}[24]. For 1900 °C and 1950 °C, the activation volume can be evaluated as 490 Å^3. Knowing both the yield strength and activation volume allows one to estimate the activation energy for the high-temperature deformation from the plot of $(\ln \sigma + \sigma V/kT)$ versus 1/T (**Figure 14**). Such efforts results in the activation energy of 1180±120 kJ/mol.

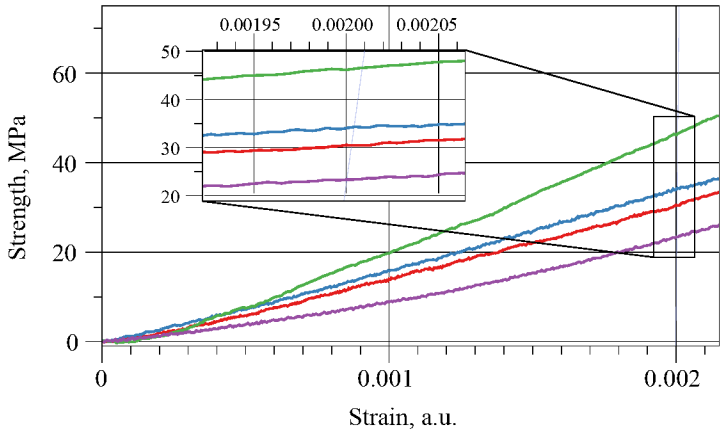

Figure 12. High-temperature deformation details at 2000 °C.

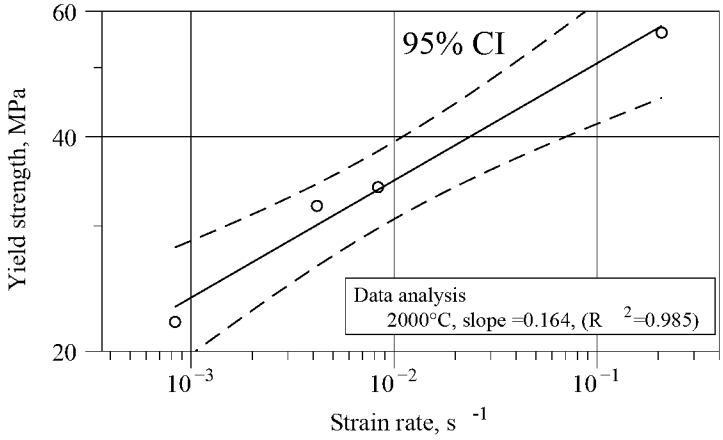

Figure 13. Effect of strain rate on 0.2 proof strength of tantalum hafnium carbide during the flexural tests at 2000 °C.

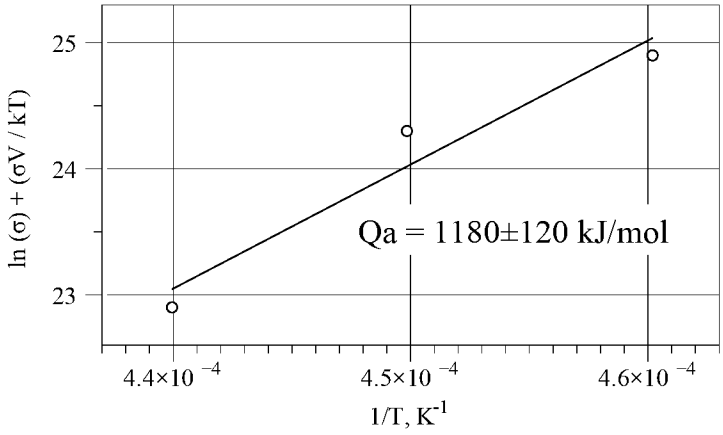

Figure 14. Evaluation of the activation energy for high-temperature deformation of $Ta_{0.2}Hf_{0.8}C$ based on the flexural tests at 1900–2000 °C.

Table 2 summarizes the creep and diffusion data by various methods for HfC and TaC [7,8,32–36]. Based on the values of the activation energy, one can presume that similar to other carbides, the values below 400 kJ/mol may indicate that diffusion of carbon in the metal (metal carbide) is the rate limiting process, while values exceeding 500 kJ/mol may indicate that the diffusion of a metal in metal (metal carbide) is the rate limiting process. Furthermore, for the high-temperature compression creep tests for $Ta_{0.25}Hf_{0.75}C_{0.94}$, Katz et al. determined the activation energy of 855±85 kJ/mol [7]. This value was the highest for the HfC–TaC carbides following an ultra-high temperature creep testing. Considering that the creep of hafnium carbide in a similar temperature range would yield 833 or 840 kJ/mol, it was concluded in [7,35,36] that creep controlled by the bulk diffusion of metal in the carbide was the rate limiting process. In [37], Ogorodnykov et al. evaluated the activation energy for the formation and migration of point defects in monolithic UHTC carbides using a model for interatomic bonding and elastic continuum. Their results for TaC and HfC are presented in **Table 3**. One can see that the results of this study are in general agreement with a metal diffusion mechanism in a carbide if a vacancy in the metal sublattice is being formed during the high-temperature deformation.

One can recall that the activation energy evaluated for the shrinkage rate observed during the SPS was 820±20 kJ/mol which is in excellent agreement with the data for the compressive creep in [7], as the spark-plasma sintering process is essentially a quasi-compressive creep test for the porous powder body. The density of the specimens for creep was between 85 and 92 % of the TD in [7], which is comparable to the relative density of the bulk during the SPS at the 2200 °C isothermal dwell (**Figure 2**).

Another factor contributing to the resistance to deformation is the grain size [7–10] because the grains coarser than 15 μm in [7–10] would mean that the bulk (lattice) diffusion mechanisms will be dominant and the contribution of the grain-boundary diffusion would be minimal. Andrievskii et al. [34] suggested that based on the diffusion profiles of ^{14}C in carbides, the contribution of the grain-boundary diffusion was at the detection limit during the creep tests above 2200 °C.

Hence, the slightly higher activation energy evaluated for the high-temperature deformation tests in flexure indicated that similar to the SPS processing, the rate limiting process should be that of metal in the carbide. Another peculiarity to consider is that the solid-solutions are known to have the possibility of a sluggish diffusion [8,32] considering a visible gap in the activation energy for the Hf in HfC and Ta in TaC (**Table 2**). At the same time, the majority of studies on carbides would consider a simple vacancy mechanism [7,34] whereas in solid-solutions the

possibility of the generation of multiple vacancies (divacancy mechanism) [38], which may lead to the decrease in the activation energy, or as shown in [37], some contribution of the interstitial atoms may lead to an increase in the activation energy. The latter is expected to be most noticeable in the case of atoms in the metal sublattice.

Conclusions

Tantalum hafnium carbide bulks were found to be difficult to consolidate as ceramics into high-density bulks that can be produced using spark-plasma sintering at temperatures exceeding 2200 °C. After the SPS, the solid-solution phase of the $Ta_{0.2}Hf_{0.8}C$ had the lattice parameter $a = 4.5719$ Å. Following the three-point flexural tests, it was observed that intergranular fracture was a dominant fracture mechanism at room temperature and was controlling the fracture behavior of the carbide specimens up to 2000 °C. Tantalum hafnium carbide showed a maximum toughness of 4.1 MPa $m^{1/2}$ at room temperature, and in general, the toughness had values of 3.4±0.4 MPa $m^{1/2}$ up to 2000 °C. At the same time, these carbides showed the adequate level of flexural strength of 600 MPa at room temperature. A high strength for $Ta_{0.2}Hf_{0.8}C$ can be observed even at 2000 °C (500±20 MPa) where these bulk showed elastic strain-stress curves. Using the data for the shrinkage rate during the SPS and the strain-stress data during high-temperature flexure, we estimated the

activation energies for the densification and flexure as 820±20 kJ/mol and 1180±120 kJ/mol, respectively. These data are in agreement with previous studies on high-temperature creep in HfC and TaC and indicate that that diffusion of the metal in the carbide lattice is the rate limiting factor. The high-temperature strength of these carbides is higher than that for monolithic or high-entropy carbides suggesting that highly creep-resistant carbides can be developed from the hafnium carbide rich solid-solutions. The observed resistance to deformation at 2000 °C for the $Ta_{0.2}Hf_{0.8}C$ ceramics may be beneficial in the designs of novel aerospace vehicles operating under extreme re-entry conditions.

References

[1] Andrievski RA, Spivak II. Strength of Refractory Compounds. Chelyabinsk:Metallurgiya; 1989. (in Russian).

[2] Kosolapova TYa. Properties, synthesis and application of refractory compounds. Reference Book. Moscow: Metallurgiya; 1986. (in Russian).

[3] Wuchina E, Opila E, Opeka M, Fahrenholtz W, Talmy I. UHTCs: Ultra-High Temperature Ceramic Materials for Extreme Environment Applications. Electrochem Soc Interface. 2007;16[4]:30–36. doi: 10.1149/2.F04074IF.

[4] Andrievskii RA, Strel'nikova NS, Poltoratskii NI, Kharkhardin ED, Smirnov VS. Melting point in systems ZrC-HfC, TaC-ZrC, TaC-HfC. Powder Metall Met Ceram. 1967;6:65–67. doi: 10.1007/BF00773385.

[5] Cedillos-Barraza O, Grasso S, Al Nasiri N, Jayaseelan DD, Reece MJ, Lee WE. Sintering behaviour, solid solution formation and characterisation of TaC, HfC and TaC–HfC fabricated by spark plasma sintering. J Eur Ceram Soc. 2016;36 [7]:1539–1548. doi: 10.1016/j.jeurceramsoc.2016.02.009.

[6] Silvestroni L, Bellosi A, Melandri C, Sciti D, Liu JX, Zhang GJ. Microstructure and properties of HfC and TaC-based ceramics obtained by ultrafine powder. J Eur Ceram Soc. 2011;31[4]:619–627. doi: 10.1016/j.jeurceramsoc.2010.10.036.

[7] Katz SM, Ordan'yan SS, Zaitsev GP. High-temperature creep in solid-solutions of the HfC–TaC system. Izd Akad Nauk SSSR, Neorg Mat. 1981;17[11]:2039–2043.

[8] Zubarev PV. High-temperature strength of the interstitial phases. Moscow: Metallurgiya; 1985. (in Russian).

[9] Katz SM, Ordan'yan SS, Goryn AI, Semenov SS, Kudryasheva LV. Effect of WC on creep of zirconium carbide. Izd Akad Nauk SSSR, Neorg Mat. 1971;15[10]:1775–1778.

[10] Avgustinik AI, Katz SM, Ordan'yan SS, Goryn AI, Kudryasheva LV. Compressive creep in ZrC–NbC solid-solutions at temperatures 2600–3150 °K. Izd Akad Nauk SSSR, Neorg Mat. 1972;7[8]:1417–1420.

[11] Demirskyi D, Vasylkiv O. Analysis of the high-temperature flexural strength behavior of B4C–TaB2 eutectic composites produced by in situ spark plasma sintering. Mater Sci Eng A. 2017;697:71–78. doi: 10.1016/j.msea.2017.04.093.

[12] Demirskyi D, Vaslykiv O. Spark plasma sintering and high-temperature strength of B6O–TaB2 ceramics. J Eur Ceram Soc. 2017;37[8]:3009–3014. doi: 10.1016/j.jeurceramsoc.2017.02.052.

[13] Darolia R, Archbold TF. Plastic deformation of polycrystalline zirconium carbide. J Mater Sci. 1976;11:283–290. doi: 10.1007/BF00551439.

[14] Borodianska H, Demirskyi D, Sakka Y, Badica P, Vasylkiv O. Grain boundary diffusion driven spark plasma sintering of nanocrystalline zirconia. Ceram Int. 2012; 38[5]:4385–4389. doi: 10.1016/j.ceramint.2011.12.064.

[15] Demirskyi D, Suzuki TS, Grasso S, Vasylkiv O. Microstructure and flexural strength of hafnium diboride via flash and conventional spark plasma sintering. J Eur Ceram Soc. 2019;39[4] 898–906. doi: 10.1016/j.jeurceramsoc.2018.12.012.

[16] Young WS, Cutler IB. Initial sintering with constant rates of heating. J Am Ceram Soc. 1970;59:659–663. doi: 10.1111/j.1151-2916.1970.tb12036.x.

[17] Ramqvist L. Hot Pressing of Metallic Carbides. Powder Metallurgy. 1966;9[17]:26–46. doi: 10.1179/pom.1966.9.17.002.

[18] Ivanko AA. The Hardness. Kyiv:Naukova Dumka;1968. (in Russian).

[19] Zhang C, Gupta A, Seal S, Boesl B, Agarwal A. Solid solution synthesis of tantalum carbide-hafnium carbide by spark plasma sintering. J Am Ceram Soc. 2017;100[5]:1853–1862. doi: 10.1111/jace.14778.

[20] Demirskyi D, Vasylkiv O. Mechanical properties of SiC–NbB2 eutectic composites by in situ spark plasma sintering. Ceram Int. 2016;42[16]:19372–19385. doi: 10.1016/j.ceramint.2016.09.110

[21] Watts J, Hilmas G, Fahrenholtz WG, Brown D, Clausen B. Measurement of thermal residual stresses in ZrB2–SiC composites. J Eur Ceram Soc. 2011;31[9]:1811–1820. doi: 10.1016/j.jeurceramsoc.2011.03.024

[22] Demirskyi D, Nishimura T, Suzuki TS, Sakka Y, Vasylkiv O, Yoshimi K. High-temperature toughening in ternary medium-entropy (Ta1/3Ti1/3Zr1/3)C carbide consolidated using spark-plasma sintering. J Asian Ceram Soc. 2020;8[4]:1262–1270. doi: 10.1080/21870764.2020.1840703.

[23] Zhang X, Hilmas GE, Fahrenholtz WG. Synthesis, densification, and mechanical properties of TaB2. Mater Lett. 2008;62[27]:4251–4253. doi: 10.1016/j.matlet.2008.06.052.

[24] Demirskyi D, Vasylkiv O, Yoshimi K. High-temperature deformation in bulk polycrystalline hafnium carbide consolidated using spark plasma sintering. J Eur Ceram Soc. under review.

[25] Feng L, Chen W-T, Fahrenholtz WG, Hilmas GE. Strength of single-phase high-entropy carbide ceramics up to 2300°C. J Am Ceram Soc. 2021;104[1]:419–427. doi: 10.1111/jace.17443

[26] Demirskyi D, Borodianska H, Suzuki TS, Sakka Y, Yoshimi K, Vasylkiv O. High-temperature flexural strength performance of ternary high-entropy carbide consolidated via spark plasma sintering of TaC, ZrC and NbC. Scr Mater. 2019;164:12–16. doi: 10.1016/j.scriptamat.2019.01.024.

[27] Lanin AG, Zubarev PV, Vlasov KP. Mechanical and thermophysical properties of materials in HTGR fuel bundles. Atomic Energy. 1993;74(1):40–44. doi.: 10.1007/BF00750973.

[28] Demirskyi D, Suzuki TS, Yoshimi K, Vasylkiv O. Synthesis and high-temperature properties of medium-entropy (Ti,Ta,Zr,Nb)C using the spark plasma consolidation of carbide powders. Open Ceramics. 2020;2:100015. doi: 10.1016/j.oceram.2020.100015.

[29] Demirskyi D, Nishimura T, Sakka Y, Vasylkiv O. High-strength TiB2-TaC ceramic composites prepared using reactive spark plasma consolidation. Ceram Int. 2016;42[1]:1298–1306. doi: 10.1016/j.ceramint.2015.09.065.

[30] Kelly A, Rowcliffe DJ. Deformation of polycrystalline transition metal carbides. J Am Ceram Soc. 1967;50:253–256. doi: 10.1111/j.1151-2916.1967.tb15098.x.

[31] Data of reference 14 cited by [13]. Martin JL, Gayet P, Costa P. Stress changes in tantalum carbide with the deformation rate and temperature (1200 and 2200C). Compt Rend Ser C. 1971;272[26]:2127–2130.

[32] Samsonov GV. Interaction between carbon and refractory metals. Moscow: Metallurgiya; 1974. (in Russian)

[33] Fromm E, Gebhardt E, Roy U. Diffusion of Carbon in the carbides of Tantalum. Z Metallk. 1966;57:808–811.

[34] Andrievskii RA, Klymentko VV, Khromov YF. Self-diffusion of carbon in transition metal carbides of IV and V group. Phys Met Metallogr. 1969;28[2]:298–303.

[35] Zagryazkin VN. On mechanism of diffusion in monocarbides of transition metals. Phys Met Metallogr. 1969;28[2]292–297.

[36] Spivak II, Klymenko VV. Investigation of diffusion defects in interstitial phases. Phys Met Metallogr. 1971;32[2]:314–317.

[37] Ogorodnykov VV, Rogovoi YuI., Point defects in monolithic cubic carbides. In: Samsonov GV, eds. Carbides and alloys based on them. Kyiv: Naukova Dumka; 1976:129–136.

[38] Manning JR. Diffusion Kinetics for Atoms in Crystals. Princeton, N.J.: D. van Norstrand Comp.; 1968.

Tables

Table 1. Details on density, grain size and flexural strength of selected UHTC carbides

Composition, mol.%[*1]	Method	Relative density,%	Mean grain size, μm	Flexural strength[*2], MPa			Ref
				RT	1800 °C	2000 °C	
$Ta_{0.2}Hf_{0.8}C$	SPS	98.3	24	583	575	506	This study
$Ti_{0.2}Ta_{0.2}Zr_{0.2}Nb_{0.2}Hf_{0.2}C$	Hot pressing	99	1±0.2	421	423	318	[25]
$Ta_{0.33}Zr_{0.33}Nb_{0.33}C$	SPS	96.8	12	426	366	139	[26]
$Zr_{0.504}Nb_{0.496}C$	Conventional sintering	94	7	300	450	430	[27]
$Ti_{0.28}Ta_{0.24}Zr_{0.24}Nb_{0.24}C$	SPS	99.3	15	560	380	–	[28]
HfC[*3]	SPS	99.6	42.5	324	350	343	[24]
TaC[*4]	SPS	~92	8–20	569	165	158	[29]

[*1]Carbon content was not evaluated study or assumed to be equal to 1.0. In ref [28] carbon content was fixed to 0.99 during the Rietveld refinement.
[*2]See **Figure 9** for data of these ceramics in the wide temperature range.
[*3]Data for 'grade C' specimen.
[*4]Reference TaC samples prepared in [29] were measured at 1800 °C and 2000 °C (single test per temperature).

Table 2. Creep and diffusion data by various methods for the TaC–HfC system

System	Method	Qa, kJ/mol	Temperature range, °C	Reference
^{14}C in α-Hf	Isotope tracing	312	1120–1760	[32]
^{14}C in β-Hf	Isotope tracing	167	1820–2130	[32]
^{14}C in Ta	Isotope tracing	415	2200–2750	[33]
^{14}C in HfC	Isotope tracing	545±45	2200–2800	[34]
^{14}C in TaC	Isotope tracing	496±50	2360–2960	[43]
Hf in HfC	Diffusion theory, HT data analysis	764	-	[35]
Ta in TaC	Diffusion theory, HT data analysis	548		[35]
$HfC_{0.98}$	Compressive creep	833*1	2400– 2700	[36]
$HfC_{0.91}$	Compressive creep	840	2500–3050	[7]
$TaC_{0.94}$	Compressive creep	780±70	2500– 3050	[7]
$Hf_{0.5}Ta_{0.5}C_{0.93}$	Compressive creep	780±70	2500– 3050	[7]
$Ta_{0.25}Hf_{0.75}C_{0.94}$	Compressive creep	855±85	2500– 3050	[7]
$TaC_{0.85\text{-}1.0}$	Creep in flexure	611±30*2	2500– 2850	[8]
$Ta_{0.2}Hf_{0.8}C$	Shrinkage rate during SPS	820±20	2000–2300	This study
$Ta_{0.2}Hf_{0.8}C$	Flexure	1190±120	1900–2000	This study

*1 Creep controlled by bulk diffusion of metal in carbide
*2 Nabarro-Herring creep, metal in carbide

Table 3. Energy for formation and migration of vacancies and interstitial atom in carbides according to [37]

Compound	Type	Metal sublattice			Carbon sublattice		
		E formation, kJ/mol	E migration, kJ/mol	Ef+m, kJ/mol	E formation, kJ/mol	E migration, kJ/mol	Ef+m, kJ/mol
TaC	vacancy	410	341	751	137	548	685
HfC	vacancy	384	320	704	128	513	641
TaC	interstitial atom	1986	68	2054	616	68	684
HfC	interstitial atom	1861	63	1924	557	63	620

Figure captions

Figure 1. Details of shrinkage behavior of the powder compact via constant rate heating experiments during spark-plasma consolidation of $Ta_{0.2}Hf_{0.8}C$.

Figure 2. Effect of dwell at 2200 °C on the relative density and lattice parameter of the $Ta_{0.2}Hf_{0.8}C$ ceramics consolidated using SPS.

Figure 3. X-Ray diffraction details of bulk tantalum hafnium carbide when compared to the original TaC and HfC powders. The peak intensity was normalized to the first peak.

Figure 4. Results on refinement of the $Ta_{0.2}Hf_{0.8}C$ bulks using the lattice parameter of 4.5719 Å.

Figure 5. The lattice constant of the solid-solution carbides in the TaC–HfC as a function of the TaC content [4,5,7].

Figure 6. Flexural strength and fracture toughness of $Ta_{0.2}Hf_{0.8}C$ as a function of the testing temperature.

Figure 7. Representative microstructures of the $Ta_{0.2}Hf_{0.8}C$ ceramics following the flexural strength tests at (a,b) room temperature, (c,d) 1600 °C, and (e,f) 2000 °C.

Figure 8. Effect of the TaC addition on fracture toughness in the TaC–HfC system.

Figure 9. Effect of temperature on flexural strength of selected ultra-high-temperature carbides [25–28].

Figure 10. Effect of TaC addition on the flexural strength at 2000 °C of the monolithic and solid-solution carbides in the TaC–HfC system.

Figure 11. Crack propagation during the flexural testing at 2000 °C for $Ta_{0.2}Hf_{0.8}C$ ceramic. Insets show a macroscopic view of the polished cross-section in the BSE mode and enlarged section of the crack arrest inside a carbide grain.

Figure 12. High-temperature deformation details at 2000 °C.

Figure 13. Effect of strain rate on 0.2 proof strength of tantalum hafnium carbide during the flexural tests at 2000 °C.

Figure 14. Evaluation of the activation energy for high-temperature deformation of $Ta_{0.2}Hf_{0.8}C$ based on the flexural tests at 1900–2000 °C.

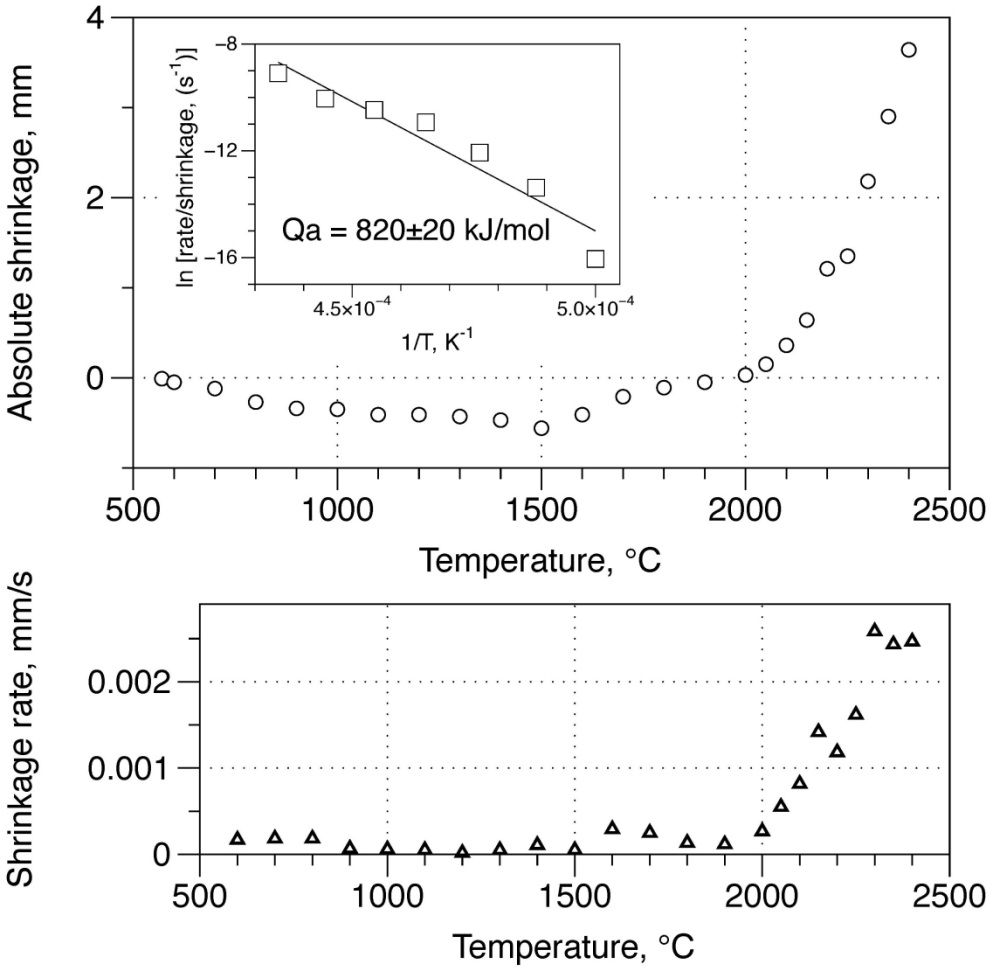

Figure 1. Details of shrinkage behavior of the powder compact via constant rate heating experiments during spark-plasma consolidation of $Ta_{0.2}Hf_{0.8}C$.

127x127mm (600 x 600 DPI)

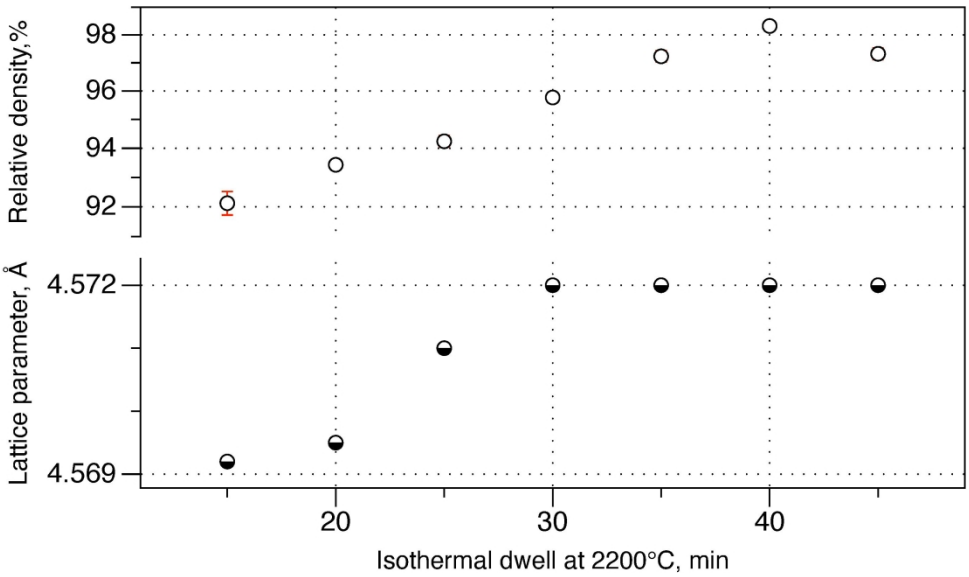

Figure 2. Effect of dwell at 2200 °C on the relative density and lattice parameter of the $Ta_{0.2}Hf_{0.8}C$ ceramics consolidated using SPS.

127x76mm (600 x 600 DPI)

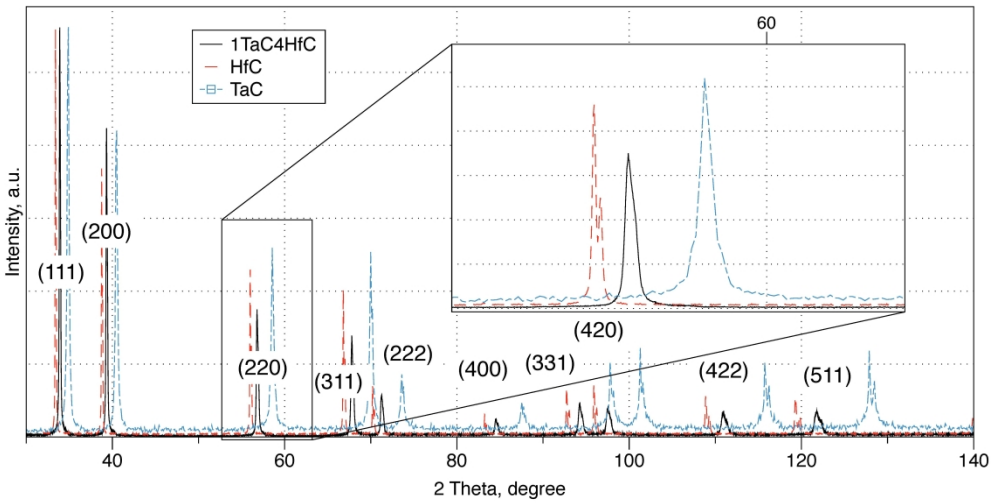

Figure 3. X-Ray diffraction details of bulk tantalum hafnium carbide when compared to the original TaC and HfC powders. The peak intensity was normalized to the first peak. The lattice parameter after the Reitveld refinement was 4.5719 Å.

225x116mm (600 x 600 DPI)

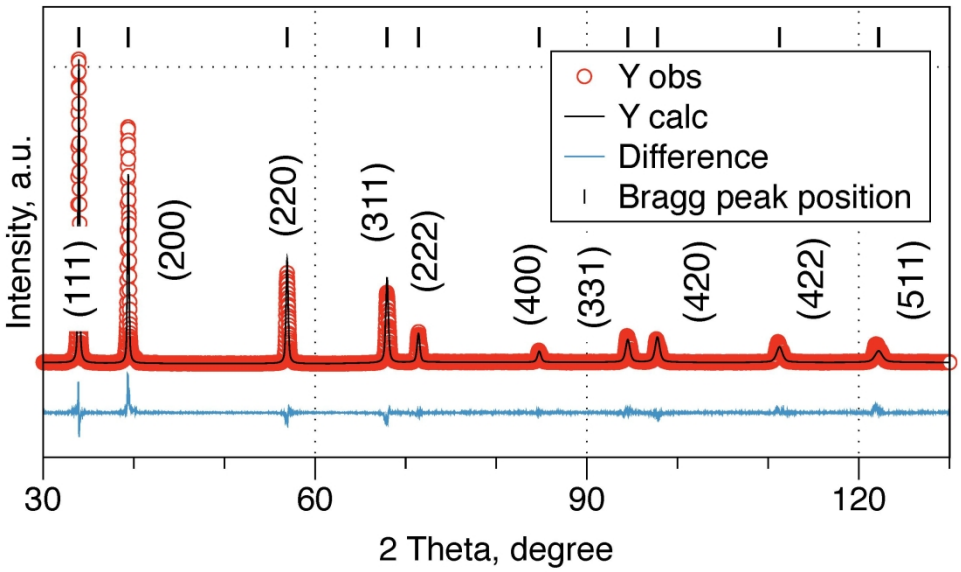

Figure 4. Results on refinement of the $Ta_{0.2}Hf_{0.8}C$ bulks using the lattice parameter of 4.5719 Å.

127x76mm (600 x 600 DPI)

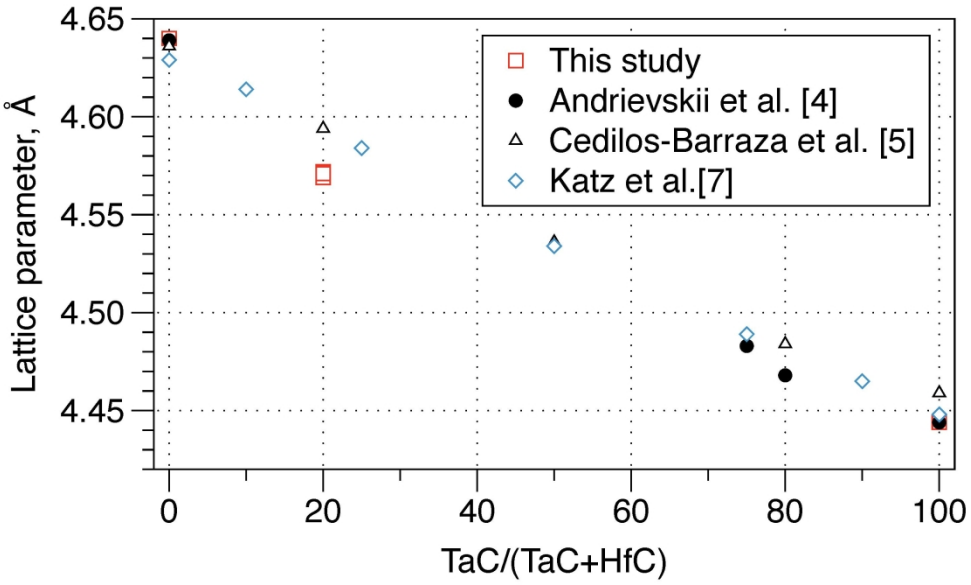

Figure 5. The lattice constant of the solid-solution carbides in the TaC–HfC as a function of the TaC content [4,5,7].

127x76mm (600 x 600 DPI)

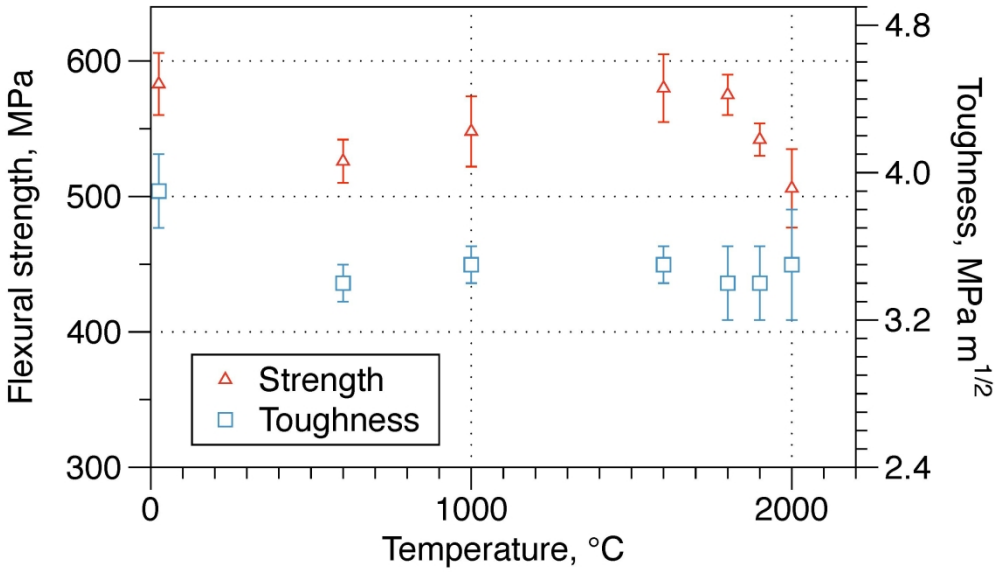

Figure 6. Flexural strength and fracture toughness of $Ta_{0.2}Hf_{0.8}C$ as a function of the testing temperature.

127x76mm (600 x 600 DPI)

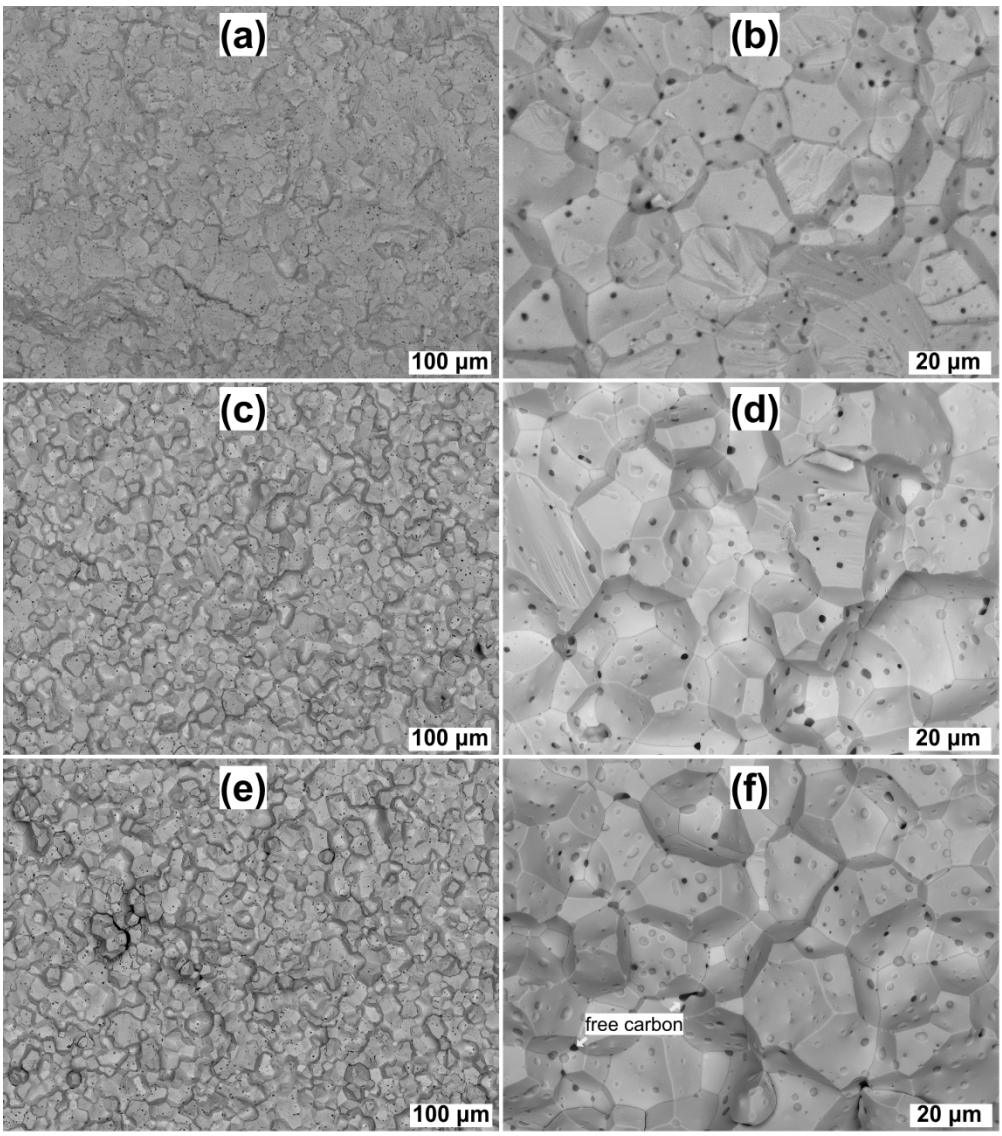

Figure 7. Representative microstructures of the $Ta_{0.2}Hf_{0.8}C$ ceramics following the flexural strength tests at (a,b) room temperature, (c,d) 1600°C, and (e,f) 2000°C.

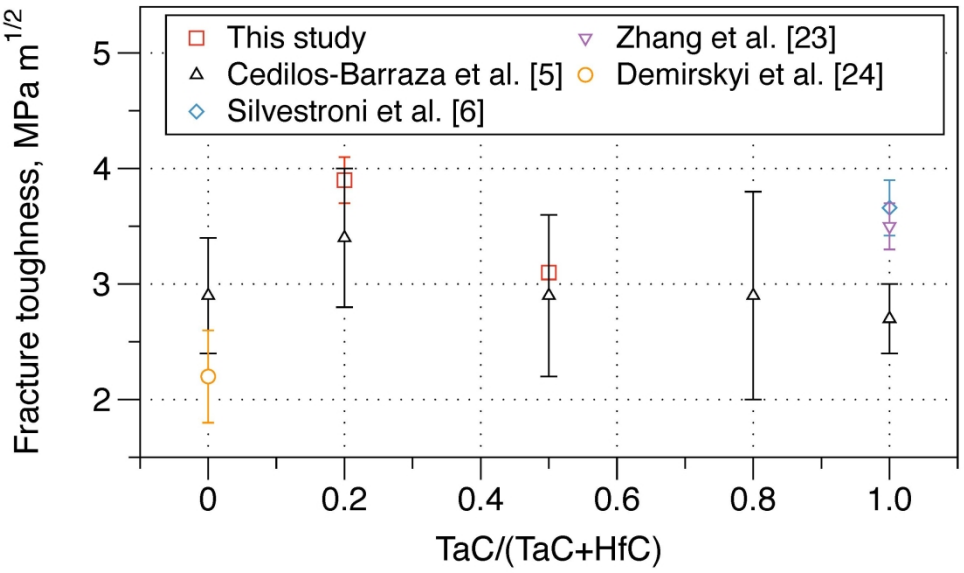

Figure 8. Effect of the TaC addition on fracture toughness in the TaC–HfC system.

127x76mm (600 x 600 DPI)

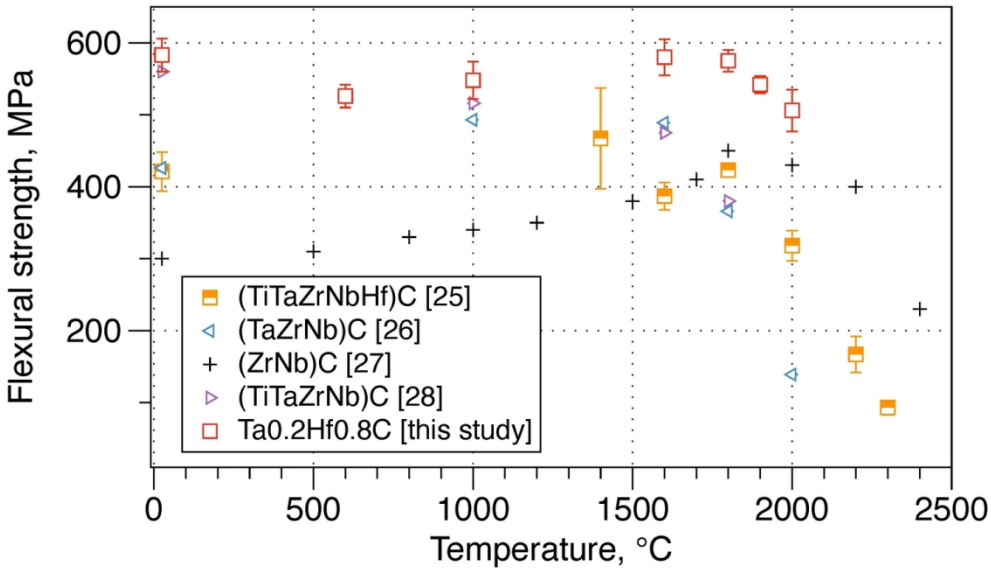

Figure 9. Effect of temperature on flexural strength of selected ultra-high-temperature carbides [25–28].

127x76mm (300 x 300 DPI)

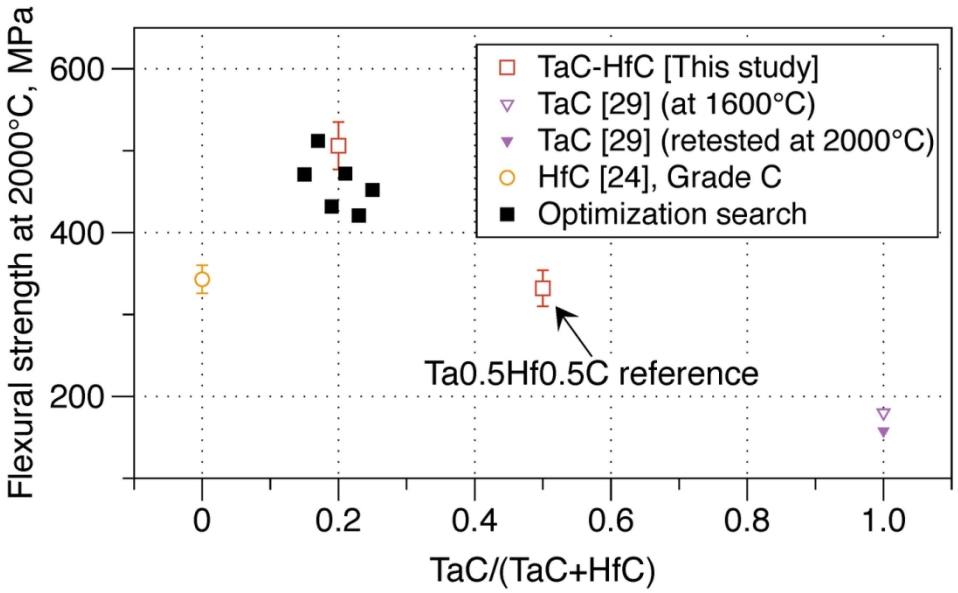

Figure 10. Effect of TaC addition on the flexural strength at 2000°C of the monolithic and solid-solution carbides in the TaC–HfC system.

127x76mm (300 x 300 DPI)

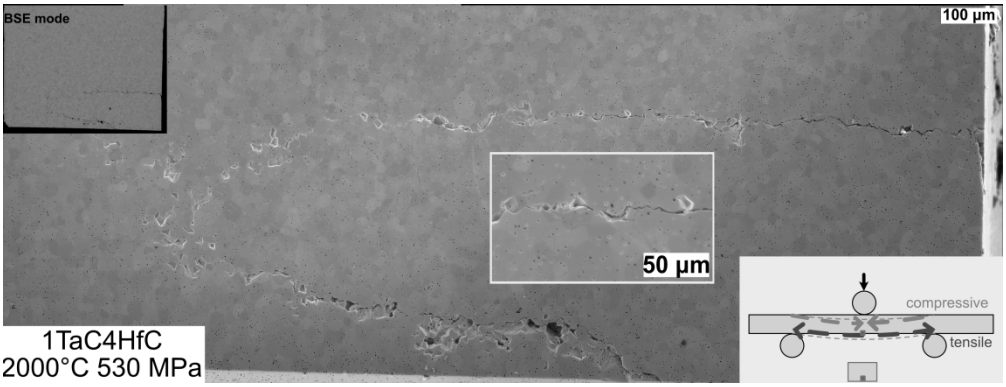

Figure 11. Crack propagation during the flexural testing at 2000°C for $Ta_{0.2}Hf_{0.8}C$ ceramic. Insets show a macroscopic view of the polished cross-section in the BSE mode and enlarged section of the crack arrest inside a carbide grain.

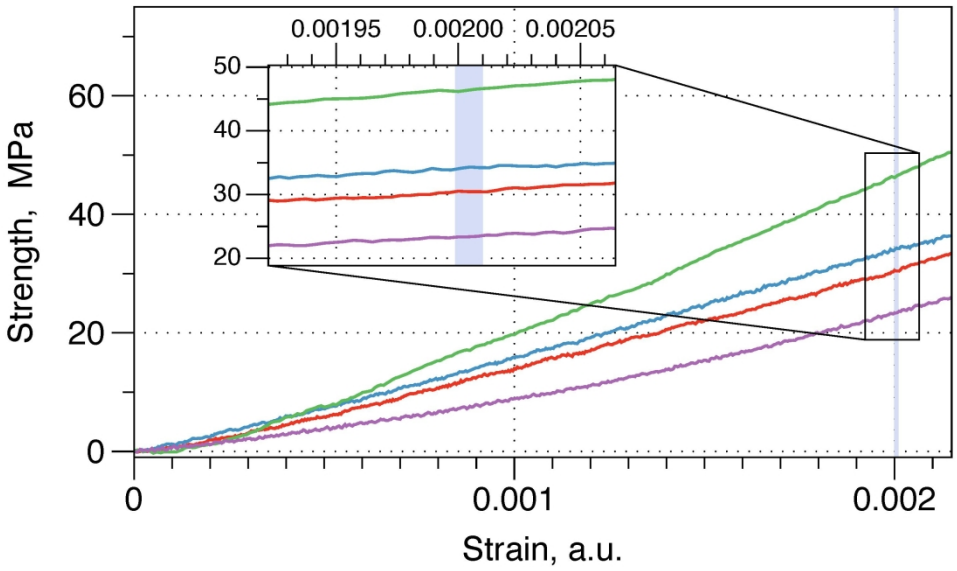

Figure 12. High-temperature deformation details at 2000 °C.

127x76mm (600 x 600 DPI)

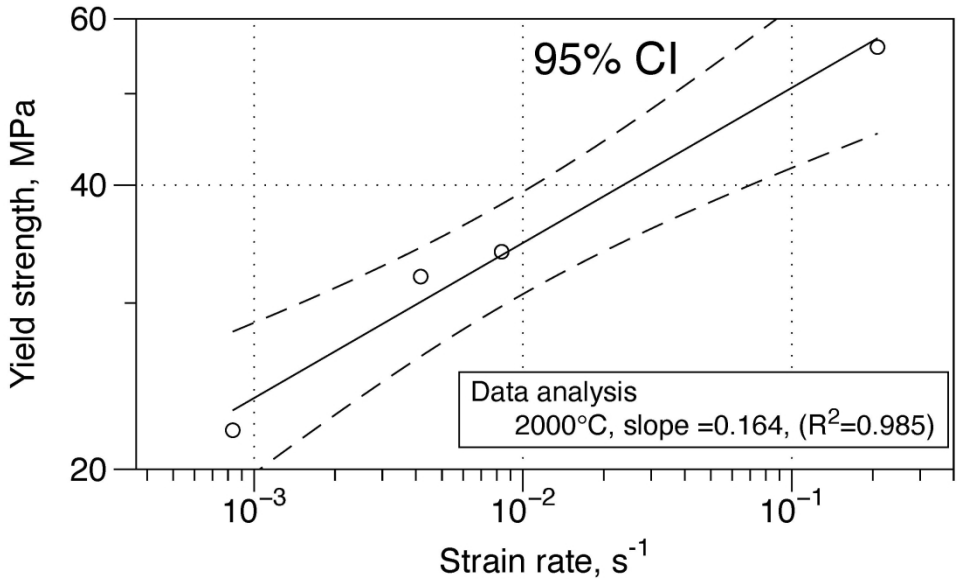

Figure 13. Effect of strain rate on 0.2 proof strength of tantalum hafnium carbide during the flexural tests at 2000°C.

127x76mm (600 x 600 DPI)

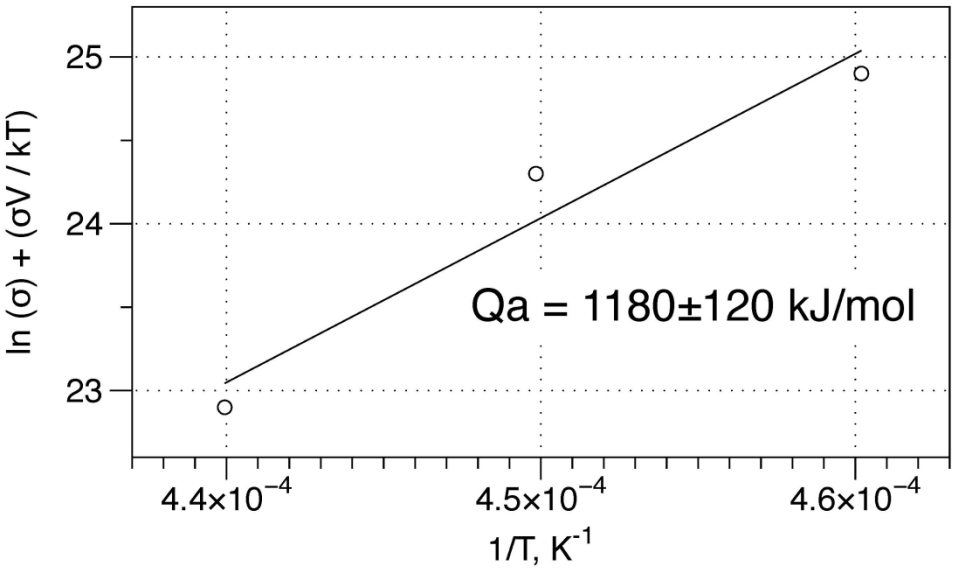

Figure 14. Evaluation of the activation energy for high-temperature deformation of $Ta_{0.2}Hf_{0.8}C$ based on the flexural tests at 1900–2000°C

127x76mm (600 x 600 DPI)

Deformation-resistant $Ta_{0.2}Hf_{0.8}C$ solid-solution ceramic with superior flexural strength at 2000 °C

D. Demirskyi (a,b,c)†, H. Borodianska (b) , T. Nishimura (b), T.S. Suzuki(b), K. Yoshimi (c), O. Vasylkiv (b)†.

(a) WPI-Advanced Institute for Materials Research (WPI-AIMR), Tohoku University, 2-1-1 Katahira, Aoba-ku, Sendai, 980-8577 Japan
(b) National Institute for Materials Science, 1-2-1 Sengen, Tsukuba, Ibaraki 305-0047, Japan
(c) Department of Materials Science and Engineering, Tohoku University, 6-6-02 Aramaki Aza Aoba, Sendai, 980-8579, Japan

Supplementary data.

In this appendix, the data concerning Energy-dispersive X-ray spectroscopy (EDS) of the oxide phase present in the $Hf_{0.8}Ta_{0.2}C$ ceramics will be presented.

An oxide phase for the $Hf_{0.8}Ta_{0.2}C$ ceramics can be identified using EDS probing of selected points in the cross-section of carbide after polishing or after the flexural tests. A typical example of EDX probing is presented in **Figure S1**. At each SEM micrograph, several probes were made. As a rule, a carbon peak was observed. This is due to the EDS depth being up to 3 μm, and the oxide inclusions occasionally had a size exceeding 3 μm in one direction. An aluminum peak was present in all specimens. This peak originated from the sample holder.

† Authors to whom correspondence should be addressed, Dmytro Demirskyi, demirskyi.dmytro.e2@tohoku.ac.jp, Oleg Vasylkiv oleg.vasylkiv@nims.go.jp

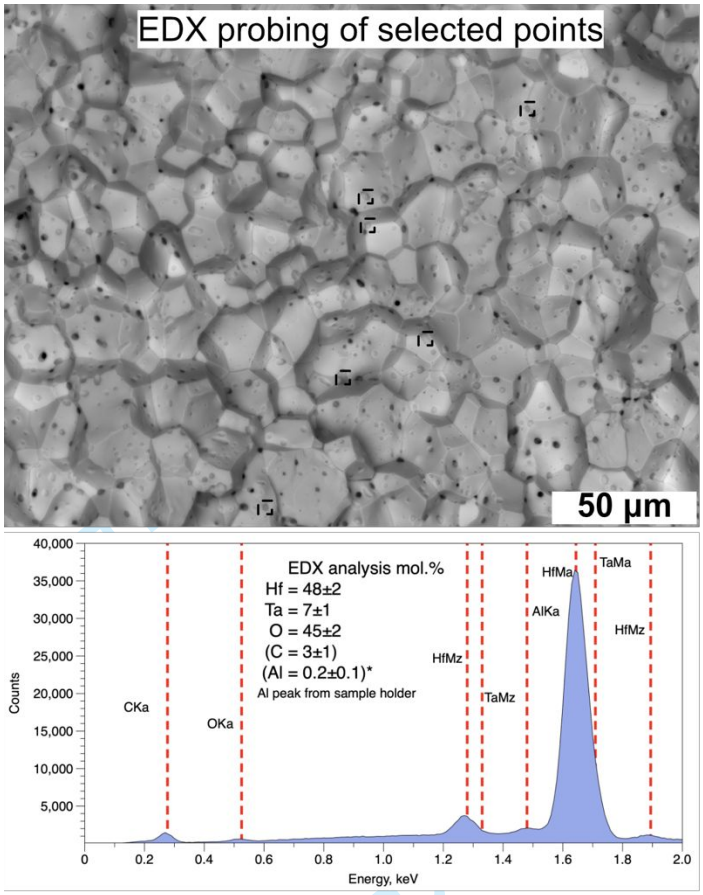

Figure S1. SEM micrographs of $Hf_{0.8}Ta_{0.2}C$ ceramics consolidated using the spark plasma method. The black phases are free-carbon and pores. Pale gray or dark gray phases were probed by EDS to determine possible phase composition.

Figure S2 summarizes the data on the EDX probes of oxide at polished and fractured specimens of the $Hf_{0.8}Ta_{0.2}C$ ceramics. It can be seen that presumed oxide phases may correspond to Ta-rich HfO_2 or HfO_2–Ta_2O_5. At selected probes, almost stoichiometric HfO_2 was identified ($\ll$ 0.5 mol.% of Ta). X-ray diffraction experiments did not reveal any oxide phase before or after the high-temperature flexural tests. Therefore it was not possible to speculate on the exact composition of

the oxide phase or its allotropic form. Selected studies [1,2] suggest that several oxides can be expected in the Ta–Hf–O system. Consolidation of $Hf_{0.8}Ta_{0.2}C$ ceramic at 2200 °C means that one should not expect the formation of the Ta_2O_5 (melting 1877±40 °C [1]). The stoichiometric hafnium oxide is known to have a higher melting point (2758±33 °C) [1]. Some binary tantalum-hafnium oxides are known to have the melting point below that of Ta_2O_5 [1,2]. In this regard, further studies on the oxidation of the ceramics in the TaC–HfC system may clarify the composition and stability of the oxide phases.

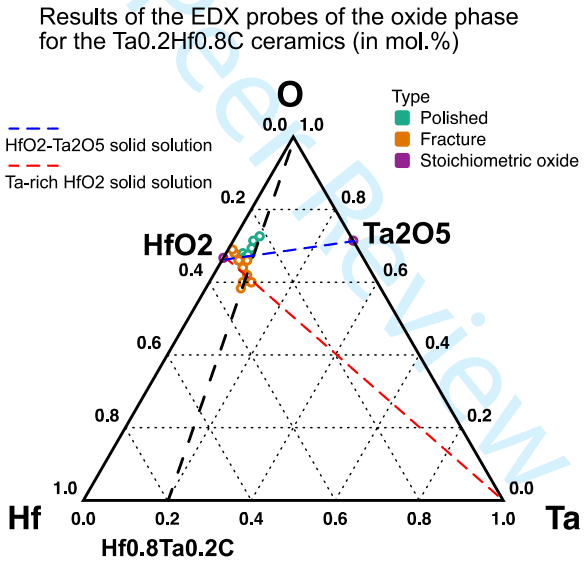

Figure S2. Chemical composition of the oxides of Hf-Ta-O ternary system observed by EDS probing of $Hf_{0.8}Ta_{0.2}C$ ceramics consolidated using the spark plasma method at 2200 °C.

[1] McCormack SJ, Tseng K-P, Weber PJK, Kapush D, Ushakov SV, Navrotsky A, Kriven WM. In-situ determination of the HfO2–Ta2O5-temperature phase diagram up to 3000°C. J Am Ceram Soc 2019;102[8]:4848–4861. doi: 10.1111/jace.16271.

[2] Perepezko JH. New Oxide Materials for an Ultra High Temperature Environment. United States. 2017. doi:10.2172/1408528.